MMD
JOURNAL / MINING.IN.UA

Studying sinkholes of the earth's surface involving radar satellite interferometry in terms of Zhezkazgan field, Kazakhstan

Aminyam Baltiyeva[1]✉ , Elmira Orynbassarova[2]*✉ , Madiyar Zharaspaev[3]✉ , Rustem Akhmetov[2]✉

[1] *D.A. Kunayev Mining Institute, Almaty, Kazakhstan*
[2] *Satbayev University, Almaty, Kazakhstan*
[3] *Kazakhmys Corporation LLP, Zhezkazgan, Kazakhstan*
Corresponding author: e-mail e.orynbassarova@satbayev.university

Abstract

Purpose is to assess the potential of radar satellite interferometry (SAR interferometry) to analyze and forecast earth's surface displacements.

Methods. The study involves the analysis of previous instrumental observations, such as high-precision levelling and seismic monitoring. The observations using global navigation satellite systems (GNSS) were carried out; satellite images were processed applying a method of sequential interferometry of persistent radar signal scatters (PS).

Findings. The research results have proved similarity between the data obtained with the help of ground instrumental methods and the data received using satellite interferometry. Two types of the earth's surface sinkholes were identified: sinkholes with smooth subsidence and hidden deformations that are not accompanied by the preliminary deformational or seismic signs. Smooth subsidence is controlled and predicted successfully with the help of the SAR interferometry methods. An algorithm has been represented to predict linear displacement trends at different time intervals involving a finite element method.

Originality. is in a complex approach of the research performance covering the following: comparative analysis of different monitoring methods, studying different sinkhole types, identifying limitations of the available methods, and proposing new approaches for more accurate and objective analysis of the earth's surface deformation within the field.

Practical implications. The research results are of practical value for rock mechanic specialists and mining operators. They can use the data to monitor and control earth's surface caving as well as provide staff safety and preserve ground infrastructure where it is possible.

Keywords: sinkholes, earth's surface, underground voids, SAR interferometry, forecast

1. Introduction

1.1. Statement of the problem and research topicality

Kazakhstan's mining industry stands as a cornerstone of the nation's economic landscape, playing a pivotal role in its development and global significance. Renowned for its vast mineral wealth, Kazakhstan boasts abundant reserves of various resources, including coal, copper, gold, and uranium [1], [2]. The mining sector has been a key driver of economic growth, attracting both domestic and foreign investments. Strategic geographical location, at the crossroads of Europe and Asia, positions it as a crucial player in the global mining arena. The industry's evolution has been marked by advancements in technology, environmental considerations, and regulatory frameworks, reflecting a commitment to sustainable development. As Kazakhstan continues to assert its presence in the international mining community, the sector's dynamism and adaptability underscore its vital role in shaping the nation's economic trajectory [3]-[5].

Radar data are being used actively for the earth's surface monitoring in many countries around the world. Such countries as England, the Netherlands, Germany, Japan, and Italy demonstrate an advanced development and modification of the methods for analyzing and interpreting the SAR interferometry data [6]-[9]. In the United States, research in the field of radar interferometry is carried out within the framework of projects of the National Aeronautics and Space Administration (NASA); the European Union performs the research in terms of the European Space Agency (ESA) [10]. As an example of active use of radar data, a study conducted before and after the famous earthquake of 2003 in the Iranian city of Bam can be mentioned [11]. The radar data processing made it possible to assess significant changes both in the earth's surface within the city-adjacent areas and destructions within the residential areas.

Many studies of earth's surface displacements during the development of mineral deposits indicate two main facts of their formation: tectonic activity and anthropogenic impact [12]-[15]. To solve this problem and assess quantitatively the displacements, monitoring tools, considering the influence of both factors, were used. These studies used successfully both static GNSS observations and permanent

GNSS stations in the daily GNSS data processing operations for regional monitoring of land displacements and active faults [16]. The stability of such a regional monitoring system is less than 1 mm per year in all three spatial coordinates. GNSS observations in the analyzed papers were integrated with the data obtained by various remote sensing methods, such as InSAR, LiDAR, and photogrammetry, into a single geodetic system, which allowed conducting successfully the interdisciplinary research [17]-[21].

Several studies address geohazard concerns, emphasizing the need for a thorough understanding of subsurface conditions to mitigate land subsidence and introduces an innovative approach for accurate landslide displacement calculation using Unmanned Aerial System survey data [22]-[24].

A joint study by the United States Geological Survey (USGS), the Sweetwater Department, and the city of San Diego [25], observing the earth's surface displacements caused by a decrease in groundwater levels, should be mentioned. The observations were also based on the interferometric synthetic aperture radar (InSAR) techniques.

Studies conducted by English scientists David Gee, Andrew Sowter et al. [26] also covered monitoring of the earth's surface deformations over oil and gas fields. As a result of these studies, deformations were detected above the deposits, and the resulting data were compared with ground measurements to assess accuracy of the results. After obtaining satisfactory results, the researchers concluded that radar images could be used successfully to solve the monitoring problems.

Earth's surface displacements during the development of mineral deposits make the formation of sinkholes one of the most pressing problems [27]-[29]. Despite the latest achievements in science and technology, forecasting the earth's surface displacements is still a complex research problem that causes difficulties in scientific and practical activities [30], [31]. In the face of the intricate challenges posed by Earth's surface displacements in tandem with mineral deposit development, the emergence of sinkholes stands out as a formidable concern. This issue not only underscores the inherent complexities in geological processes but also emphasizes the need for innovative solutions. Despite the remarkable strides in science and technology, the accurate prediction of these surface displacements remains elusive, presenting persistent obstacles to both scientific inquiry and practical applications [32]-[35]. This paper explores the potential of radar satellite interferometry (SAR interferometry) for the analysis and prediction of the Zhezkazgan field sinkholes.

The underground voids of Zhezkazgan field are a large-scale problem of the formation of sinkholes and fractures on the earth's surface. Over the entire period of the Zhezkazgan field operation, about 390 million m^3 of underground voids were formed (more than 1200 excavation units, panels, blocks, drifts, flexures etc.), including 51.6 million m^3 of the development mine workings [36], [37]. By 2022, 192 million m^3 of voids have been abandoned by uncontrolled caving, backfilling of mined-out space, and re-development. Currently, the scale of the remaining risks is 40%, which is determined by 150 million m^3 of open voids supported by pillars. Of the remaining 625 uncaved and non-abandoned excavation units, there is no access to 26% of them for inspection and determining the actual condition.

Having entered the active phase of deformation and destruction, the undermined rock mass at Zhezkazgan field undergoes irreversible processes. These processes are caused primarily by the interchamber pillars (ICP) breaking because of prolonged standing, exceeding the maximum period. Figure 1 demonstrates a process of breaking of inter-chamber pillars over time. The images were taken by the geomechanical service of Kazakhmys Corporation LLP and represent clearly the change in the ICP state starting from its original form and in the following periods of time: after 25-30 years, after 30-35 years; after 35-40 years; up to 50 and over 50 years.
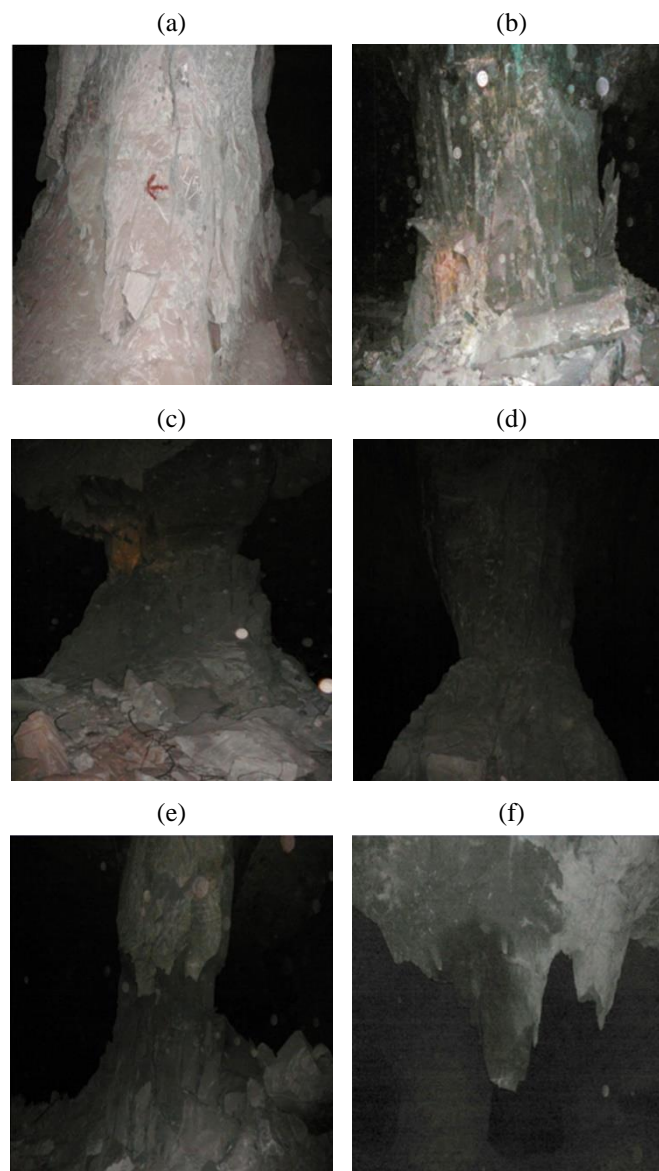
(a) (b)

(c) (d)

(e) (f)

Figure 1. A process of interchamber pillar degradation over time: (a) original appearance of the interchamber pillar; (b) type of intrachamber pillar after 25-30 years; (c) appearance of the interchamber pillar after 30-35 years; (d) condition of the intrachamber pillar after 35-40 years; (e) appearance of an interchamber pillar within the first 50 years of its standing; (f) interchamber pillar over 50 years old, with complete breaking

Unfavourable deformation processes, which remained previously beyond the forecast, began to appear at the field. The areas previously separated by panel, barrier, and interchamber pillars experience their merging. This led to several large cavings of the overlying strata with the outcropping. The geomechanical service calculated the risks of technogenic earthquakes during the instantaneous caving of weakened (unstable) sections at Zhezkazgan field. According to the re-

sults, the technological earthquake strength can reach: up to 7 points at the caving epicentre, covering an area of 70 km^2; 6 points – at a distance of 5 km over an area of 340 km^2; and 5 points – it will spread over a distance of 10-12 km.

According to sources [38], [39], it is impossible to prevent the current process of pillars' breaking without additional measures to maintain a stable geomechanical situation. Large-scale cavings on the surface will occur inevitably, accompanied by the technogenic earthquakes.

The topicality of this study is determined by the following: preserving the life and health of people; possibility of transferring equipment, ground infrastructure; and calculating the risks of a technogenic earthquake.

1.2. Purpose and tasks of the study

The purpose of the study is to determine the capabilities of SAR interferometry, with the emphasis on its applicability, reliability, and ability to provide reliable data for determining complex processes of the earth's surface displacements occurring within Zhezkazgan field. Two cases of caving were selected as the objects of study: a sinkhole with smooth subsidence and a sinkhole with hidden deformations. To achieve the goal, following tasks were completed: comprehensive geodynamic monitoring, comparative analysis of the results obtained, verification of the SAR data, algorithm for calculating subsidence of linear displacement trends for various time intervals using the finite element method.

2. Materials and methods

2.1. Sinkholes of the earth's surface with hidden deformations and smooth subsidence

In terms of the study, the sinkholes were selected that can be classified according to following nature of deformations: with hidden deformations – sudden caving without previous deformation and seismological signs; and smooth subsidence – with slow and smooth displacements of the earth's surface as a result of gradual rock caving.

2.1.1. Sinkhole of the earth's surface with hidden deformations

The caving under study occurred at Vostochnyi mine in October 9, 2020; it was the outcropping one. The total area of the formation is 140×100 m^2. A sudden and dangerous earth's surface movement characterizes this sinkhole. Based on the results of a mining and geological analysis, the potentially unstable zones closest to the sinkhole were identified (Fig. 2).

The sinkholes were zoned according to weakening zones (a), zones of several mining levels (b), and available tectonic disturbances (c). It should be noted that no information has been preserved within the sinkhole territory concerning the availability of mined-out spaces as the surveying plane tables burnt during the fire. The opportunity to develop a digital model of voids using secondary documents in the archive (survey plans on tracing paper, lavsan) was missed.
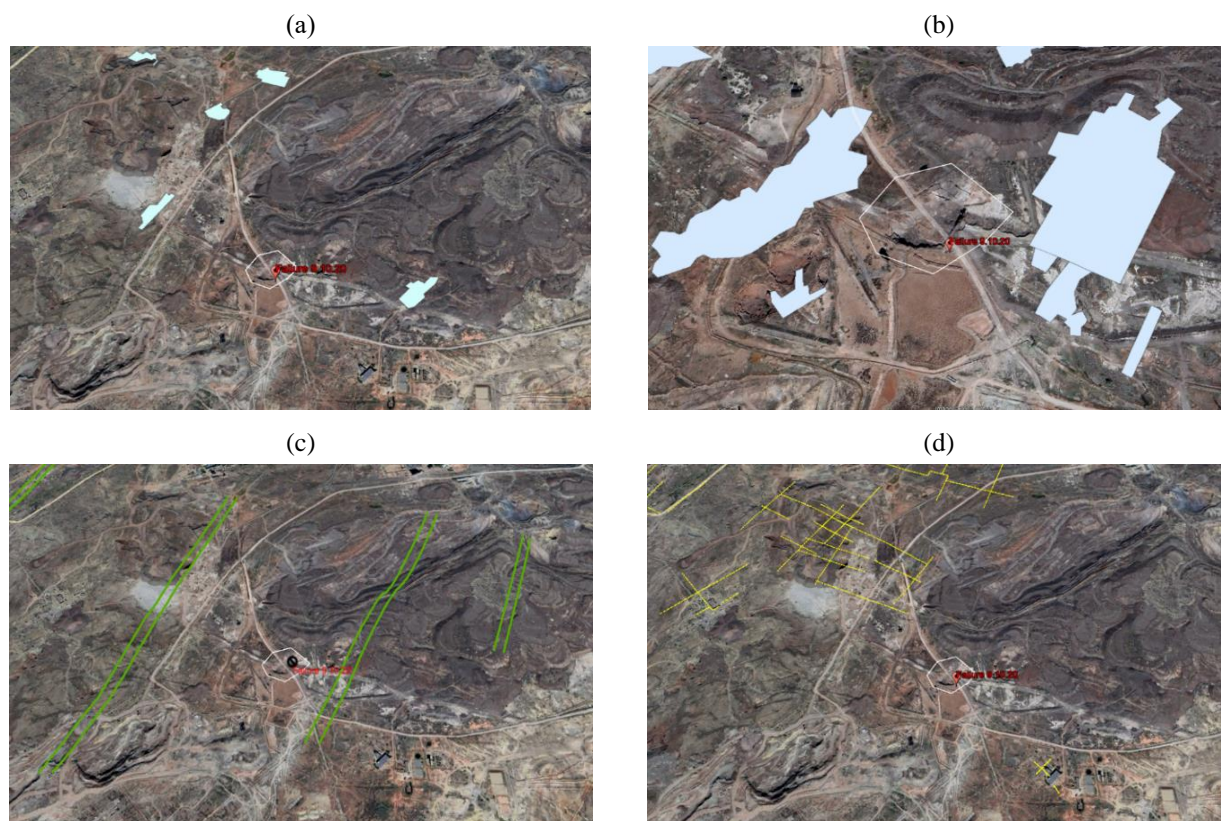

Figure 2. Location of the sinkhole and potentially unstable zones: (a) depleted zones; (b) redevelopment; (c) flexures; (d) profile lines

Therefore, a "green" corridor with ground infrastructure was built within this area, which subsequently experienced its caving. In addition, Figure 2d shows that there are no profile lines over the sinkhole area. In such cases, SAR interferometry is the only possible research method.

2.1.2. Sinkhole with smooth subsidence of the earth's surface

This caving of the overlying strata above the mined-out spaces occurred in January 2020, 3.5 km west of the previous sinkhole; it was the outcropping one in the form of a smooth trough.

Smooth subsidence over a long period of time makes it easy to detect using X-ray diffraction methods as well as to carry out various experimental calculations to predict it. Figure 3 shows photos before and after the caving.
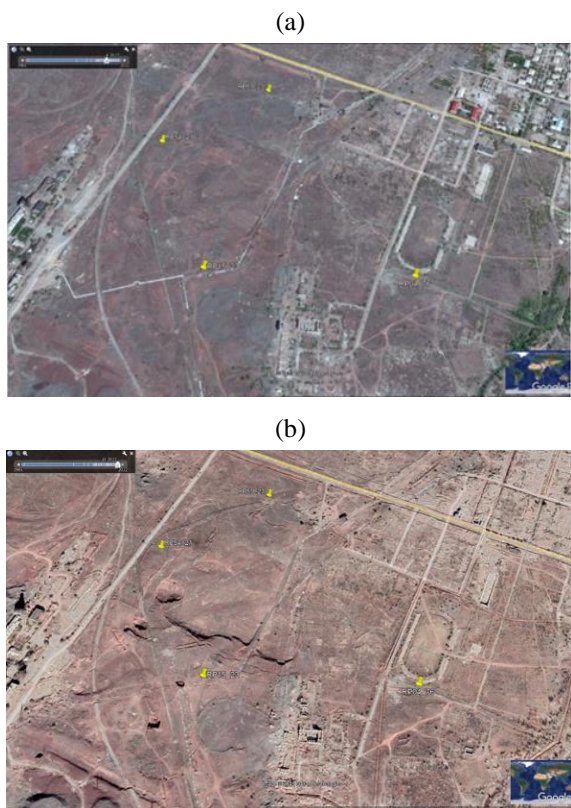
(a)

(b)

Figure 3. Sinkhole with a smooth subsidence of the earth's surface: (a) image before the subsidence formation; (b) image after the subsidence formation

Currently, a process of after-caving and displacement of the overlying strata continues. The Geomechanical Department plans abandon this area by uncontrolled caving to stabilize the geomechanical situation.

2.2. Monitoring and instrumental observations

Comprehensive monitoring is carried out within the territory of Zhezkazgan field involving such methods as: high-precision levelling, GNSS observations, seismic monitoring, and satellite image processing using satellite radar interferometry. Each type of monitoring has different resolution, extent, advantages, and limitations, showing some differences in measurement points [40]. Therefore, at the beginning, the results of each method were determined individually; then comparisons were made between the different methods to obtain a unique, consistent interpretation of the controlled movements.

2.2.1. High-precision levelling

To monitor deformation processes at Zhezkazgan field, periodic instrumental observations are carried out. High-precision levelling is applied as instrumental observations, which is currently being performed along 126 profile lines. There were a total of 146 profile lines with a total length of 42 km. High-precision levelling involves DNA03 levelling units. Observations are carried out annually; in some sections of profile observation lines they are performed several times a year.

In general, after 25 years of repeated development of pillars, the grouping of profile lines was reduced greatly due to caving of the overlying strata. Many new areas, as well as the caving area under consideration, have no profile lines. Therefore, in terms of this study, the analysis was complemented by the data from the benchmarks of the preserved profile line, being the closest one to the caving.

2.2.2. GNSS observations

Our group started GNSS observations of a geodynamic state of the Zhezkazgan field territory in June 2021 to be able to verify SAR interferometry data and obtain horizontal displacement vectors. The first cycle of measurements was carried out immediately after the completion of reconnaissance operations. Satisfactory results of the processing of the GNSS data from the first cycle confirmed the optimal location of GPS antennas in accordance with the multipath effect. Basing on the geodynamic ground, four cycles were performed at 23-24 geodetic points, combined with the existing profile lines for high-precision levelling (Table 1).

Table 1. GNSS observations in terms of a geodynamic ground of Zhezkazgan deposit

Cycle	Period	Volume	Number of sessions
1	June 14-17, 2021	24 points	6
2	October 4-7, 2021	24 points	6
3	May 3-6, 2022	24 points	8
4	September 12-15, 2022	23 points	8

Since monitoring of the deformation processes requires the highest accuracy in determining the deformation parameters [26], [41], GNSS equipment of geodetic class Leica GPS1200, GS16, and Smartstation were used to perform measurements. Figure 4 shows the Leica GS16 GNSS equipment and the benchmark.
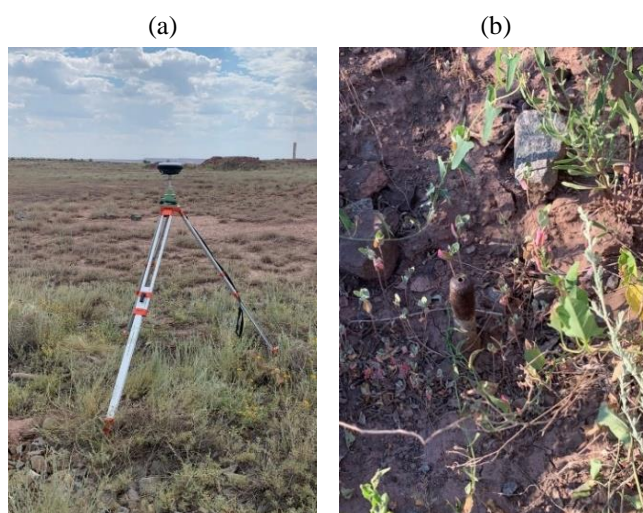
(a)   (b)

Figure 4. GNSS station within the territory of Zhezkazgan field

6-8 measurement sessions were performed in each cycle at the field, depending on the number of available instruments. Observations were carried out in a static mode, duration of a synchronous session was at least 5 hours with a recording interval of 15 seconds and an exceed mask of 10º. At the end of the observation session, the receivers were moved to the next measurement points. In this case, the GPS antennas were centred over the levelling points, orienting the

north marker to 0º magnetic azimuth. When placing GPS antennas, data on the equipment used (type and serial number of the receiver and antenna) and antenna height were entered into the field journal. This information was used in the subsequent cycles of GNSS measurements for using systematic instruments at the observation points.

GNSS data were processed using the GAMIT/GLOBK software package, version 10.71, developed at Massachusetts Institute of Technology [42]. GAMIT stands for "GPS At MIT", it can be used to estimate station position, atmospheric delays, satellite orbits, and Earth orientation parameters. GLOBK, meaning "Global Kalman filter", uses finite GAMIT solutions and other types of post-processed solutions with full covariance matrices to estimate station positions, velocities, time series, and many other estimates. Unlike commercial software, GAMIT/GLOBK produces a network solution of highly defined International GNSS Service (IGS) stations. The global network avoids assumption concerning stability of some areas of the field for processing the local network [43].

Horizontal displacements were calculated between the cycles based on the coordinates of GNSS points in the UTM 42 N projection. The displacements of GNSS points in mm during the period between the first and second measurement cycles as well as the second and fourth ones, based on the GAMIT/GLOBK solution, are shown in Figure 5.
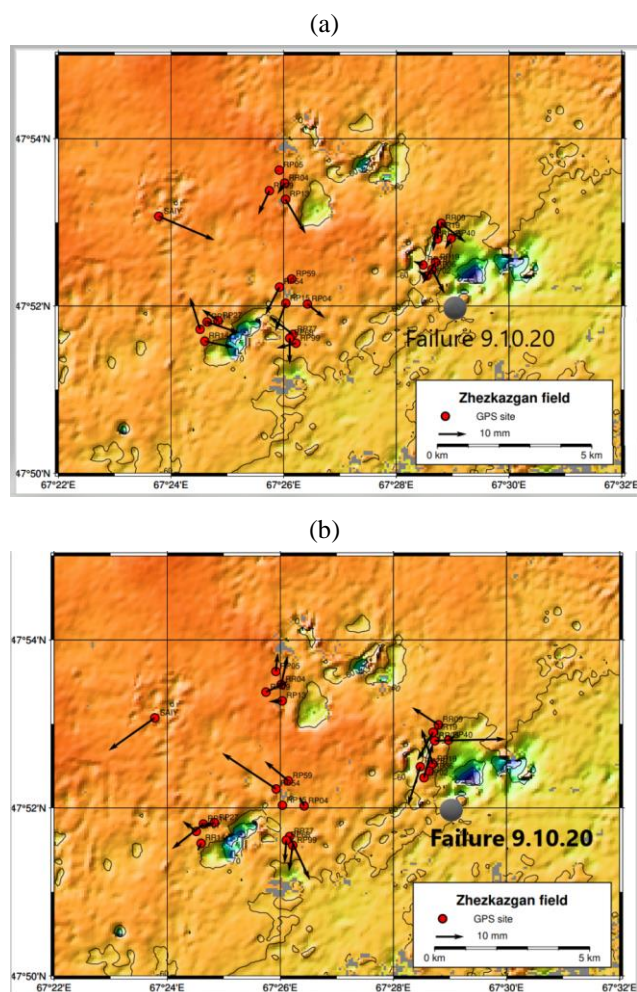
(a)

(b)

Figure 5. Horizontal displacement vectors according to GNSS observations: (a) June – October 2021; (b) October 2021 – September 2022

The horizontal movements of GNSS points are multidirectional, suggesting that local geophysical signals, such as uplift and subsidence, cause horizontal expansion and contraction [44], [45]. The overall sceptical error in the planned coordinates of the points can exceed 5 mm, taking into account an error in centring GNSS antennas [46]. Deformations during the period of October 2021 – September 2022 are less affected by seasonal factors of the earth's surface movement; thus, it can be assumed that the vectors of horizontal displacements are caused by production work at the field and the associated accuracy of GNSS measurements. Along with an increase in the time interval between cycles, there is a simultaneous increase in the maximum values of the horizontal component of movements of individual GNSS points as well as the average value of the horizontal component for the entire field.

2.2.3. Seismic monitoring

Beginning from 2007 to the present, the ISSI/IMS seismic system (South Africa/Australia) with 20 seismic sensors has been operating at the field. Seismograms are processed by the order of Kazakhmys Corporation LLP. At 19:12 of 10/09/2020, the ISSI system recorded a seismic event (SE) with the energy of $E = 102.8$ J. This event was attributed to the boundary of the previously caved (in 2009) area of panels and old workings; therefore, this SE did not indicate the beginning of a dangerous situation. The point of this SE is 350 m away from the place where caving occurred on 10/09/2020. The analysis of "raw" seismograms made it possible to find 9 weak SEs within this area that preceded the caving. In October 9, at 8 a.m., the "landslide"-type SE appeared without a sharp signal entry; thus, those signals were classified as an interference. A comparison between a typical seismic event and a landslide-type seismic event is represented in Figure 6 (X-axis is time; Y-axis is amplitude, expressed in micrometers per second). The signal of a typical SE is the high-frequency one. The moments of arrival of longitudinal and transverse waves are visible on the seismograms, and SE signal of a "landslide" type is long-lasting, low-frequency, and does not have clear arrivals.

A mechanism of rock mass breaking is a gradual weakening of the layers of red-coloured weak rocks as they become saturated with moisture and flow of water to the lower levels, right up to the roof of the mine working under study. This can explain the "soft" subsidence/caving of the overlying strata of this area without seismic signals, accompanied usually by the development of discontinuous fractures in the mass.

In general, predicting the "landslide"-type seismic events before they occur remains a challenge for modern science. There are various methods and approaches for studying and predicting earthquakes. However, currently there are no reliable and accurate ways to predict caving with a high degree of confidence.

2.2.4. SAR interferometry

Sentinel-1 synthetic aperture radar data was used to study the earth's surface displacement. The basic principle of radar interferometry is processing of images received from interferometric satellites. These satellites operate with different parameters, such as resolution, wavelength, and frequency of surveying in terms of one area. The data quality is influenced by spatial resolution and such factors as atmospheric and ionospheric interference, vegetation, snow cover etc. [17], [47], [48].
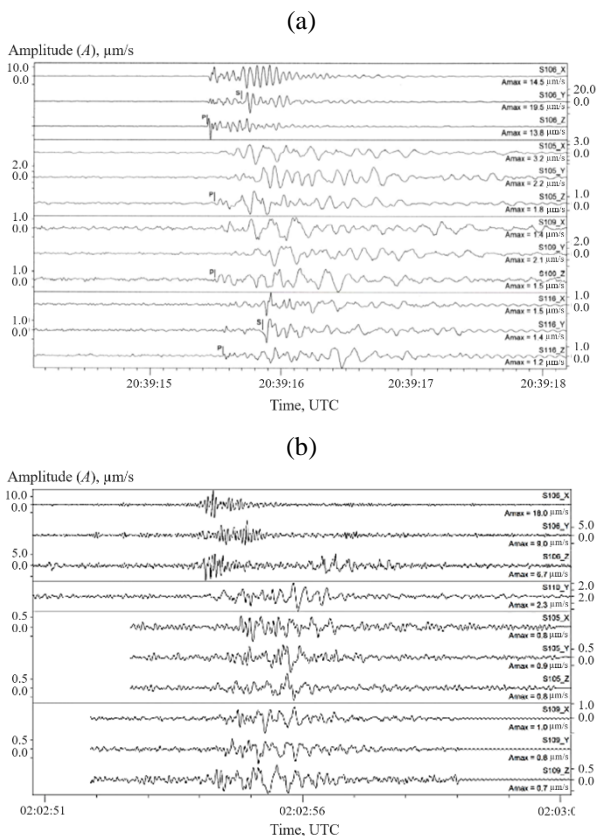
(a)

(b)

Figure 6. Seismograms of the typical- and "landslide"-type SEs: (a) typical seismic event; (b) seismic event of the "landslide" type

The images were processed using a method of sequential interferometry of permanent scatterers of the radar signal (PS) more than two times using different processing parameters in the Sarproz software (from 2019 to 2021). Figure 7 shows the boundaries of image processing.

After downloading the images, additional orbital data files corresponding to each image were downloaded to improve accuracy and remove orbit-related errors. Then a master image was selected, and coregistration was performed.

Figure 8 shows the interferometric configuration of the images used for the analysis, where x-axis indicates the temporal baseline and y-axis indicates the perpendicular baseline. It should be noted that almost all baselines for S1 images are controlled accurately within a maximum distance of 100 m. With a smaller spatial/temporal baseline, as in our case, higher spatial coherence is usually achieved. Each point in the image represents SAR survey, and each line represents one interferogram.

After successful coregistration, the next steps are as follows [49], [50]:
– making a reflectivity map;
– developing the maps of amplitude stability indices;
– selecting the candidates for permanent scatterers (PSC);
– deploying the phase of a multiple-element network cut;
– assessing and removing the atmospheric phase;
– reading a PS phase and estimating the displacement.
The motions of PS targets are extracted as a function of time relative to the selected basic image.

Reflectivity map. A reflectivity map is the first processing output that shows what the SAR image looks like and gives an overview of the backscatter characteristics of the SAR signal within its area under study. A reflectivity map is generated by averaging the amplitude of all images in the stack.
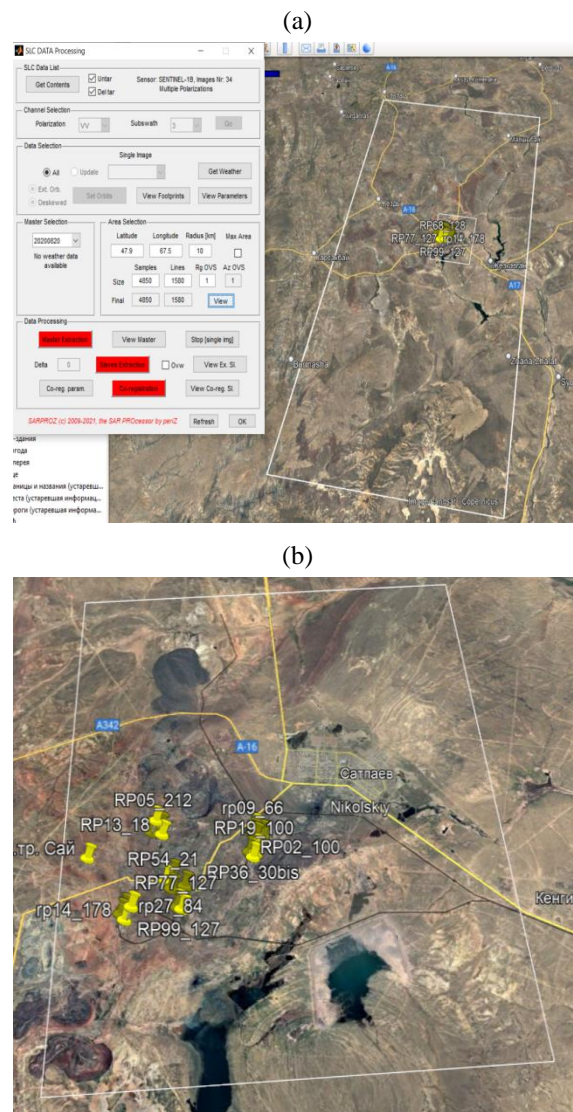
(a)

(b)

Figure 7. Boundaries of image processing using the PS method: (a) boundaries of the satellite image coverage; (b) boundaries of the processing and location of benchmarks for GNSS observations
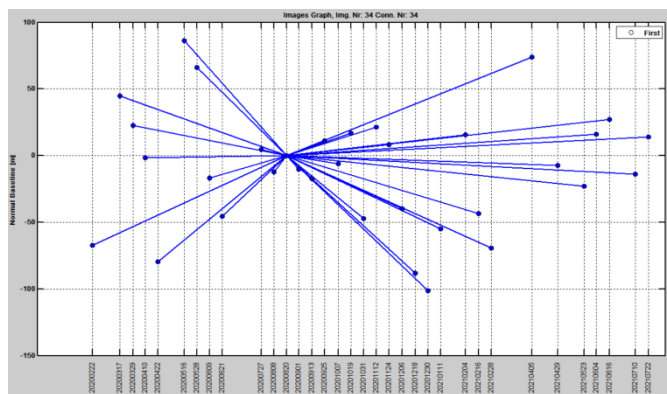

Figure 8. Interferometric configuration of the images

Figure 9 demonstrates a reflectivity map of its one entire frame. The program selected the control point automatically.

Shuttle Radar Topography Mission (SRTM) was applied to remove a topographic error. SRTM is a spacecraft mission that aims to create a digital elevation model (DEM, Fig. 10) of the Earth using radar technology. SRTM was launched in 2000 and has provided valuable data for many uses, including topographic error removal in radar interferometry.

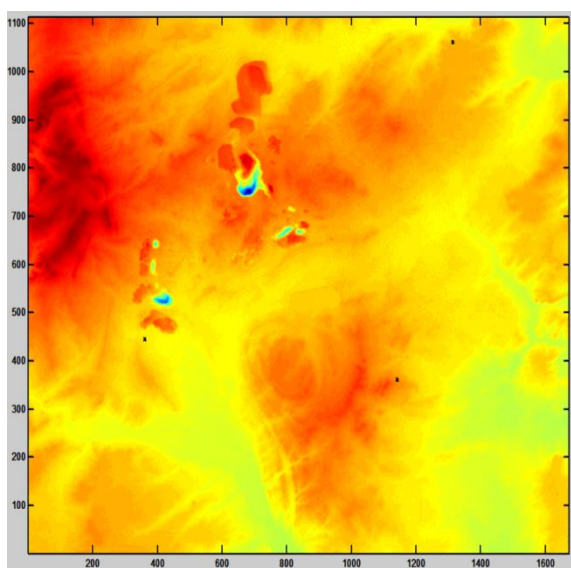*Figure 9. Reflectivity map and control point*

Figure 10. Digital elevation model (DEM)

The use of SRTM to remove a topographic error in SAR interferometry has following features and advantages:

– high resolution of DEM: SRTM has created DEM with a resolution of about 30 meters for the most part of the Earth. This improves significantly the data quality compared to more approximate DEMs that were used before;

– global coverage: SRTM covers most of the Earth's surface between the 60th north and 56th south parallels, making it useful for a variety of applications in different regions;

– vertical accuracy: DEM generated by SRTM, has high vertical accuracy, which is important for accurate measurements of the earth's surface displacements.

A topographic error removal process in radar interferometry using SRTM typically involves following steps:

– interferometric data processing: the radar data acquired at two different moments of time are processed to create an interferogram. This interferogram contains information about phase differences between the two measurements;

– filtering and processing of the interferogram: interferograms may contain various errors and noise, therefore filtering and processing methods are used to improve the data quality;

– phase decoding and topographic error removal: using SRTM DEM, the phase information in the interferogram is corrected taking into consideration the topographic error. This is done by subtracting the phase information created by the topography from the interferogram;

– analysis of the results: after removing the topographic error, the interferogram is analyzed to measure displacements of the earth's surface or other parameters of interest.

Overall, using SRTM DEM to correct topographic errors allows for more accurate and reliably interpreted results in radar interferometry, which is useful in many applications, including monitoring the earth's surface displacements and terrain changes.

Average velocity map. Using the PS method, the point vector files were created to illustrate visually certain changes in the earth's surface displacements. These point vector files contain information about the average displacement rates obtained after deep processing of the original data set. Figure 11 is a snapshot of these displacements; it records the earth's surface state for the period of 2021.
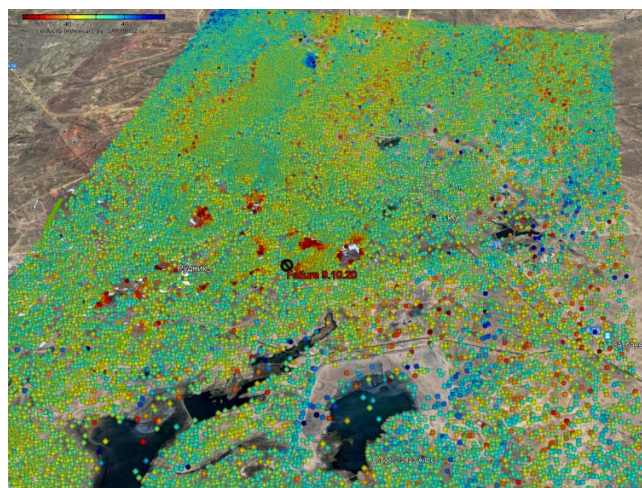

Figure 11. Map of the Zhezkazgan field displacements

The PS method is a highly efficient technique for the earth's surface monitoring that relies on stable retroreflection points. It makes it possible to analyze changes and movements of the earth's crust at certain points with high accuracy and time resolution.

The point vector files generated by PS show the location of stable points and store information on displacement at those points over the period under study. This is especially valuable when tracking deformations.

The displacement map for 2021 shown in Figure 11 is an important result of the visualization and analysis of the data. It helps identify the areas with the greatest changes; besides, it is used in predicting potential events associated with the earth's surface deformation.

There are more than 11000 points on the map, each of which is a stable reflector and contains a number of characteristics, including geographic coordinates, average displacement rates, date, coherence level, and other parameters. Active subsidence zones are defined by colour gradation from dark orange to dark bordeaux; on average, they are 80 mm/year (green and light blue dots – stable surface, yellow – up to 30 mm/year).

3. Results

3.1. Collective results of the study in terms of sinkhole with hidden deformations

3.1.1. Results of SAR interferometry

Data processing for 2019 has showed generally the stability of the points; for 2020, it has demonstrated insignificant subsidence values, being up to 10 mm (Fig. 12), which may be within the accuracy of the method.
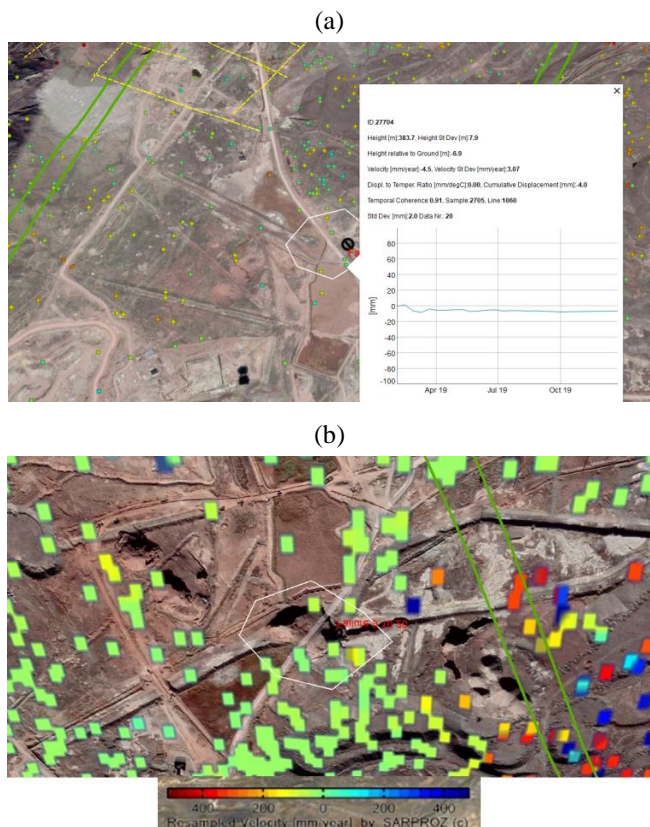
(a)

(b)

Figure 12. Results of SAR interferometry preceding the sinkhole: (a) displacement dynamics during the period from February to December 2019; (b) interpolation of the results of SAR interferometry for the year of 2020

The obtained results of SAR and seismic monitoring did not show the development of intensive processes of the earth's surface subsidence and seismic events preceding the caving. Therefore, this caving occurred without previous deformation and seismological signs can be characterized as a sinkhole with hidden deformations.

According to the SAR interferometry data for 2021 (Fig. 13), when a sinkhole had been already formed, fluctuations in the elevations within ±5 mm were recorded with a general subsidence trend with an average annual rate of 35 mm/year.
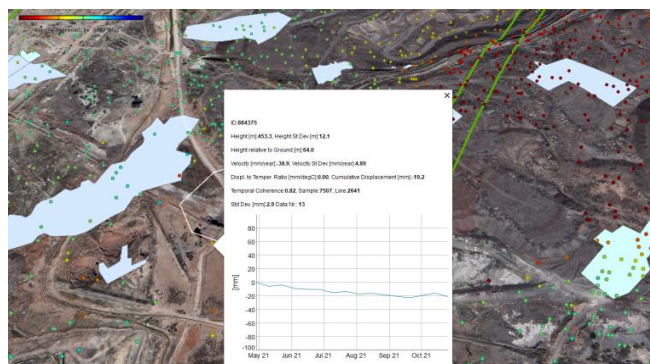

Figure 13. Dynamics of displacements after caving

Only 6 SAR points fell on this caving area of 140×100 m²; that indicates a shortage of coordinate points during intense subsidence. In general, even such a small number of SAR points confirm the continuation of subsidence of the caved area; it is the safest method for monitoring a possible increase in the caving boundaries.

3.1.2. Results of monitoring the profile line being closest to the sinkhole

The profile lines of high-precision levelling have not been preserved within the area where the sinkhole occurred. Therefore, the benchmark data from the closest preserved profile line 100 (about 500 m) were added for the analysis.

The subsidence dynamics for each of the benchmarks for the period from 2018 to 2022, represented in Fig. 14a, was analyzed. Figure 14b shows the dynamics of SAR interferometry points for 2019 and 2021, falling on profile line 100.
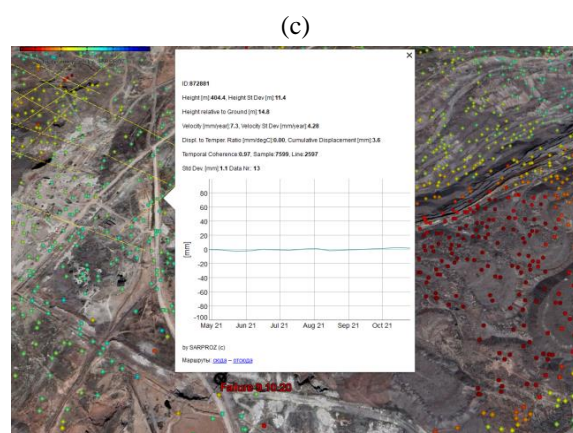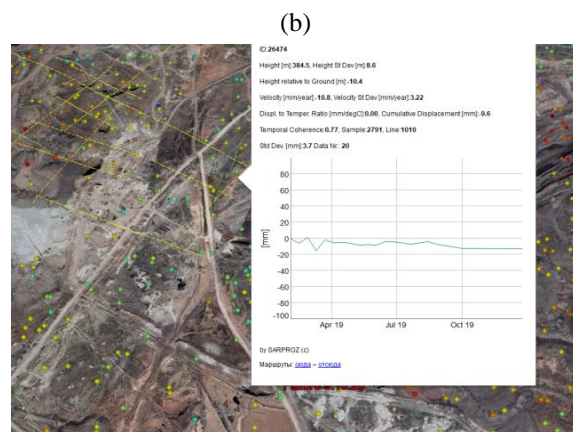
(a)

(b)

(c)
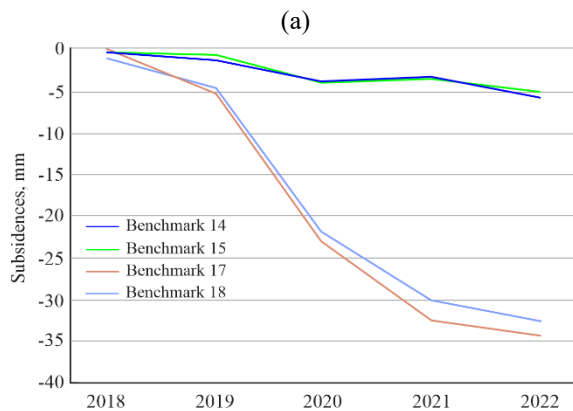
Figure 14. Ground-based and satellite data of the profile line 100: (a) high-precision levelling 2018-2022; (b) InSAR interferometry (February – December 2019); (c) InSAR interferometry (May – November 2021)

In general, while comparing the two observation methods for this period, the following can be noticed: slight subsidences in 2019, both according to the levelling data and according to the SAR interferometry data, and stabilization of fluctuations in 2021 (Table 2).

Table 2. Results of the displacements of high-precision levelling and SAR interferometry for 2019 and 2021

Period	High-precision levelling	SAR-interferometry
2019	subsidence within the limits of 1.5-5.2 mm	subsidence within the limits of 5-15 mm
2021	subsidence within the limits of 0.4-10 mm	Fluctuations within the limits of 3-4 mm

There is no displacement dynamics of the points on profile line 100 according to the SAR interferometry data for 2020.

A clearer picture can be seen if you build a graph showing the joint dynamics of the benchmarks Rp. 14, Rp. 15, Rp. 17, Rp. 18, and Rp. 19, which are closest to the sinkhole along profile line 100. Figure 15 shows that the peak of the greatest subsidence for all the benchmarks under consideration occurred precisely in 2020 (from 14 to 18 mm/year).
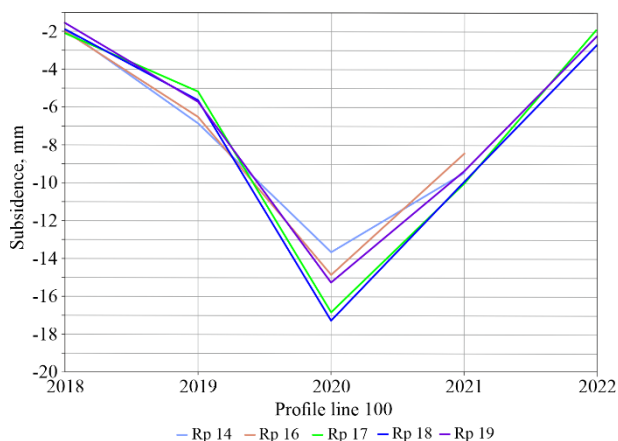

Figure 15. Sinkhole based on high-precision levelling of profile line 100

Levelling on this profile line is performed once a year; measurements were taken in August 10, 2020, 2 months before the formation of the sinkhole under study. In general, the obtained values are not critical for the average annual velocity; but due to the large frequency of observations, it is not known that this subsidence occurred during the entire period or closer to the date of caving.

3.1.3. Results of the SAR method verification

To provide the reliability of the SAR method application in terms of this study, verification and joint interpretation of the data results with the results of ground-based instrumental measurements were performed. Consider as an example Rp. 19 of profile line 100 as we have the levelling data and GNSS observations for this benchmark; and the SAR interferometry points fall close to it as well.

Figure 16 shows the GNSS observation data for Rp. 19 in a 5-hour static mode (June 2021 – September 2022), high-precision levelling data (October 2018 – June 2022), and satellite interferometry data (February 2019 – December 2019; May 2021 – October 2021). There is a continuing subsidence trend with minor fluctuations and good convergence between the three observation methods. According to the levelling data for 2019, a subsidence of more than 1 cm occurred; a similar average annual rate is shown by the results of interferometry, with the possibility to see fluctuations of a point throughout the year. During 2020, interferometry did not detect a point near this benchmark. For 2021, according to the GNSS observations and satellite interferometry data, a slight rise was recorded from May to October. Unlike SAR, levelling does not detect such fluctuations in the earth's surface and shows only the average annual speed due to the long frequency of observations (in this case, it is once a year).
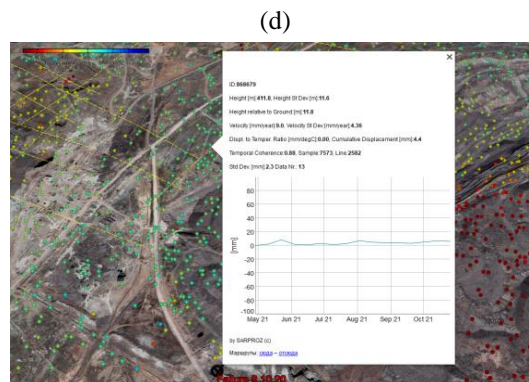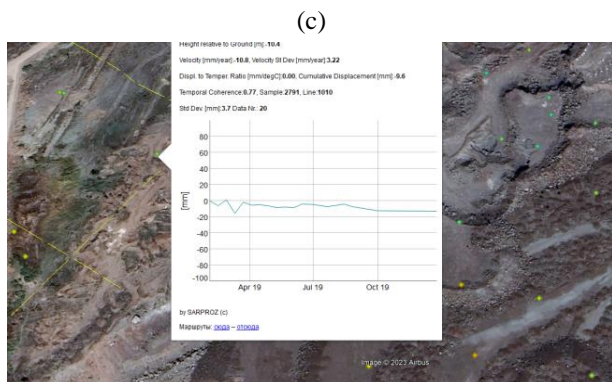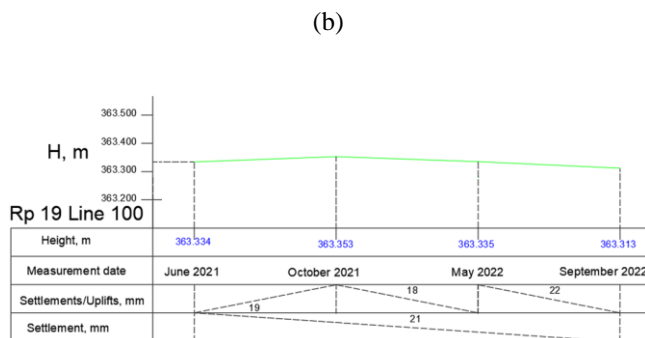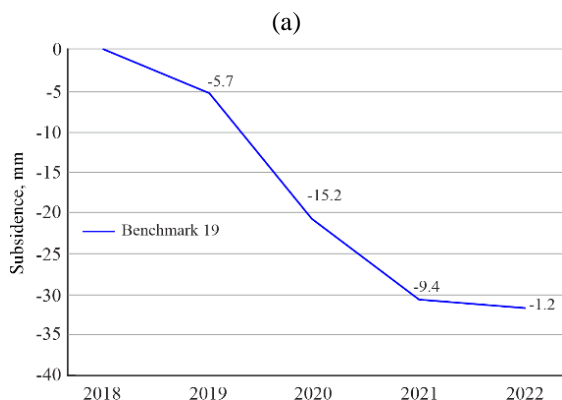
(a)

(b)

(c)

(d)

Figure 16. Verification of the InSAR data with ground measurements: (a) dynamics of high-precision levelling for Rp. 19 (October 2018 – June 2022); (b) dynamics of the GNSS observations for Rp. 19 (June 2021 – September 2022); (c) dynamics of the SAR point close to Rp. 19 (February 2019 – December 2019); (d) dynamics of the SAR point close to Rp. 19 (May 2021 – October 2021)

According to source [42], it has been established in recent decades that under the influence of horizontal tectonic stresses at the boundaries of the displacement trough (as well as in the displacement trough itself), both horizontal compression deformations and uplifts (instead of subsidence) can equally occur.

3.2. The SAR interferometry results and forecast for a sinkhole with smooth subsidence

Interferometry handled the formation of sinkholes with smooth subsidence perfectly and showed clearly the displacement trends of each point. The most dangerous displacement trend is a progressive type of deformation (a subsidence rate increases over time), which can be predicted from the time of caving by calculating the parameters of inverse velocities. The inverse velocity method is a time-series analysis method that is used to predict rock caving and rock slides. It is based on taking into account the rock movement velocity before and after the caving. The main principle of the method is to assume the following: at the moment of caving, the rock movement velocity reaches its maximum value; after that, it begins to decrease. By analyzing the obtained data, the method helps determine the probability of new caving occurring at a certain period of time. The disadvantage of the inverse velocity method is that it does not consider the influence of external factors and their changes over time.

The finite element method (FEM) is used to simulate numerically the earth's surface behaviour over time, including the prediction of linear displacement trends. However, it should be noted that FEM itself is not a method for analyzing trends or time series. Instead, FEM is used to solve differential equations that describe the earth's surface behaviour; it involves calculations at different points in time. For each moment of time, a numerical solution of differential equations is performed for each finite element. This makes it possible to determine the earth's surface movements at different points in time.

If you know critical values of the displacements, then this method makes it possible to calculate the moment of time that falls under this value. Figure 17 shows dynamics of SAR points, which fell on the surface of sinkhole with smooth earth's surface subsidence with an average annual speed of 100 mm/year, for using the FEM method. Then, a calculation algorithm for point 28439 is given (Fig. 17a).

For each i element, we have following subsidence data represented in Table 3.

Table 3. Subsidence data for each i element

1 ($i = 1$)	2 ($i = 2$)	3 ($i = 3$)
$u1[1] = 29.3$ mm	$u1[2] = 28.5$ mm	$u1[3] = 22.1$ mm
$u2[1] = 20$ mm	$u2[2] = 27.8$ mm	$u2[3] = 12.5$ mm
$u3[1] = 31.4$ mm	$u3[2] = 16.3$ mm	$u3[3] = 20.8$ mm

Develop a system of equations for each element i to find the values for coefficients $k1[i]$, $k2[i]$, and $k3[i]$, where $t1$, $t2$, $t3$, $t4$, and $t5$ are the time intervals between subsidence measurements: $t1 = 0$ days, $t2 = 101$ days, $t3 = 84$ days, $t4 = 85$ days, and $t5 = 85$ days (Table 4).

Solve each of the equation systems to find the values for coefficients $k1[i]$, $k2[i]$, and $k3[i]$ for each i element, substituting the values of time intervals and subsidence (Table 5).

After solving the systems of equations, we obtain the values of the coefficients for each i element (Table 6).
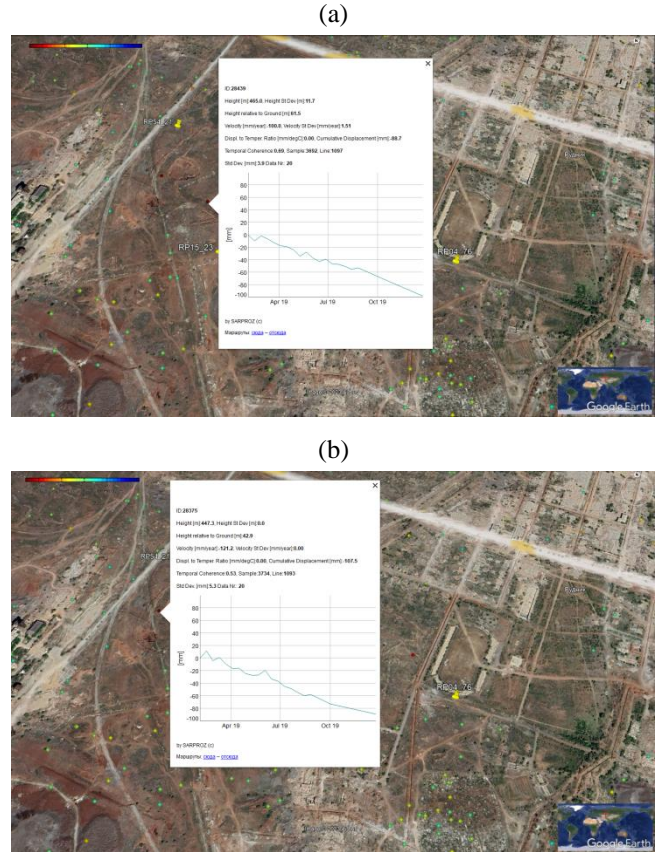

(a)

(b)

Figure 17. Interferometric SAR (InSAR) data for the period of February to December 2019: (a) subsidence dynamics of point 28439; (b) subsidence dynamics of point 28375

Table 4. Systems of equations for each i element

1 ($i = 1$)
$k1[1] \cdot t1 + k2[1] \cdot t2 + k3[1] \cdot t3 = u1[1]$
$k1[1] \cdot t2 + k2[1] \cdot t3 + k3[1] \cdot t4 = u2[1]$
$k1[1] \cdot t3 + k2[1] \cdot t4 + k3[1] \cdot t5 = u3[1]$
2 ($i = 2$)
$k1[2] \cdot t1 + k2[2] \cdot t2 + k3[2] \cdot t3 = u1[2]$
$k1[2] \cdot t2 + k2[2] \cdot t3 + k3[2] \cdot t4 = u2[2]$
$k1[2] \cdot t3 + k2[2] \cdot t4 + k3[2] \cdot t5 = u3[2]$
3 ($i = 3$)
$k1[3] \cdot t1 + k2[3] \cdot t2 + k3[3] \cdot t3 = u1[3]$
$k1[3] \cdot t2 + k2[3] \cdot t3 + k3[3] \cdot t4 = u2[3]$
$k1[3] \cdot t3 + k2[3] \cdot t4 + k3[3] \cdot t5 = u3[3]$

Table 5. Finding the values of coefficients k1[i], k2[i], and k3[i] for each i element

1 ($i = 1$)
$k1[1] \cdot 0 + k2[1] \cdot 101 + k3[1] \cdot 84 = 29.3$
$k1[1] \cdot 101 + k2[1] \cdot 84 + k3[1] \cdot 85 = 20$
$k1[1] \cdot 84 + k2[1] \cdot 85 + k3[1] \cdot 85 = 31.4$
2 ($i = 2$)
$k1[2] \cdot 0 + k2[2] \cdot 101 + k3[2] \cdot 84 = 28.5$
$k1[2] \cdot 101 + k2[2] \cdot 84 + k3[2] \cdot 85 = 27.8$
$k1[2] \cdot 84 + k2[2] \cdot 85 + k3[2] \cdot 85 = 16.3$
3 ($i = 3$)
$k1[3] \cdot 0 + k2[3] \cdot 101 + k3[3] \cdot 84 = 22.1$
$k1[3] \cdot 101 + k2[3] \cdot 84 + k3[3] \cdot 85 = 12.5$
$k1[3] \cdot 84 + k2[3] \cdot 85 + k3[3] \cdot 85 = 20.8$

To forecast the sinkhole formation at a certain point of time, using the obtained values of coefficients $k1[i]$, $k2[i]$, and $k3[i]$ for each i element, we can substitute the values of time intervals $t1$, $t2$, $t3$, $t4$, and $t5$ into the corresponding equations.

Table 6. Values of the coefficients for each i element

1 ($i = 1$)		
$k1[1] \approx 0.000232$	$k2[1] \approx 0.30603$	$k3[1] \approx -0.04182$
2 ($i = 2$)		
0.001141	$k2[2] \approx 0.21814$	$k3[2] \approx -0.04731$
3 ($i = 3$)		
0.005889	$k2[3] \approx 0.089497$	$k3[3] \approx -0.016666$

For example, for element 1 ($i = 1$) we substitute the values of time intervals and the values of the coefficients that we found earlier (Table 7).

Table 7. Calculating subsidence for element 1 (i = 1)

1 ($i = 1$)
$k1[1] \cdot t1 + k2[1] \cdot t2 + k3[1] \cdot t3 = u1[1]$
$k1[1] \cdot t2 + k2[1] \cdot t3 + k3[1] \cdot t4 = u2[1]$
$k1[1] \cdot t3 + k2[1] \cdot t4 + k3[1] \cdot t5 = u3[1]$
Values of time intervals
$0 \cdot k1[1] + 101 \cdot k2[1] + 84 \cdot k3[1] = 29.3$
$101 \cdot k1[1] + 84 \cdot k2[1] + 85 \cdot k3[1] = 20.0$
$84 \cdot k1[1] + 85 \cdot k2[1] + 85 \cdot k3[1] = 31.4$
Values of coefficients
$0 \cdot 0.000232 + 101 \cdot 0.30603 + 84 \cdot (-0.04182) \approx 29.3$
$101 \cdot 0.000232 + 84 \cdot 0.30603 + 85 \cdot (-0.04182) \approx 20.0$
$84 \cdot 0.000232 + 85 \cdot 0.30603 + 85 \cdot (-0.04182) \approx 31.4$

Subsidences are also calculated for other time intervals. Take following interval $t6 = 150$ days for the calculation (Table 8).

Table 8. Calculating subsidence for 150 days

$t6 = 150$ days	$k1[1] \cdot t4 + k2[1] \cdot t5 + k3[1] \cdot t6 = u4[1]$
Values of time intervals	$k1[1] \cdot 85 + k2[1] \cdot 85 + k3[1] \cdot 150 = u4[1]$
Values of coefficients	$0.000232 \cdot 85 + 0.30603 \cdot 85 + (-0.04182) \times$ $\times 150 = 0.01972 + 26.06355 - 6.273 = 19.80927$

Preliminary calculation of the displacements has showed a further 19.8 mm subsidence after 150 days. There are no dynamics of displacements of the points for this sinkhole for 2020 but the dynamics of displacements for 2021 shows continuation of the linear trend of subsidence (Fig. 18).

Thus, we can predict subsidence for various time intervals using the values of coefficients $k1[i]$, $k2[i]$, and $k3[i]$, which were obtained after solving the equation systems for each i element. This allows the method to predict surface behaviour and potential sinkhole formation based on the available subsidence and time interval data using SAR interferometry. This forecast method must be supplemented with certain qualitative characteristics. To develop full-fledged forecast algorithms, a number of numerical and experimental calculations should be carried out, for which retrospective satellite interferometry data are excellent.

4. Discussion

Comprehensive monitoring is carried out within the territory of Zhezkazgan field; the monitoring involves various methods, including high-precision levelling, GNSS observations, seismic monitoring, and satellite image processing using satellite radar interferometry. Each monitoring method has its own characteristics, including resolution, extent, advantages, and limitations. This results in certain differences in the measurement points and data obtained by each method.
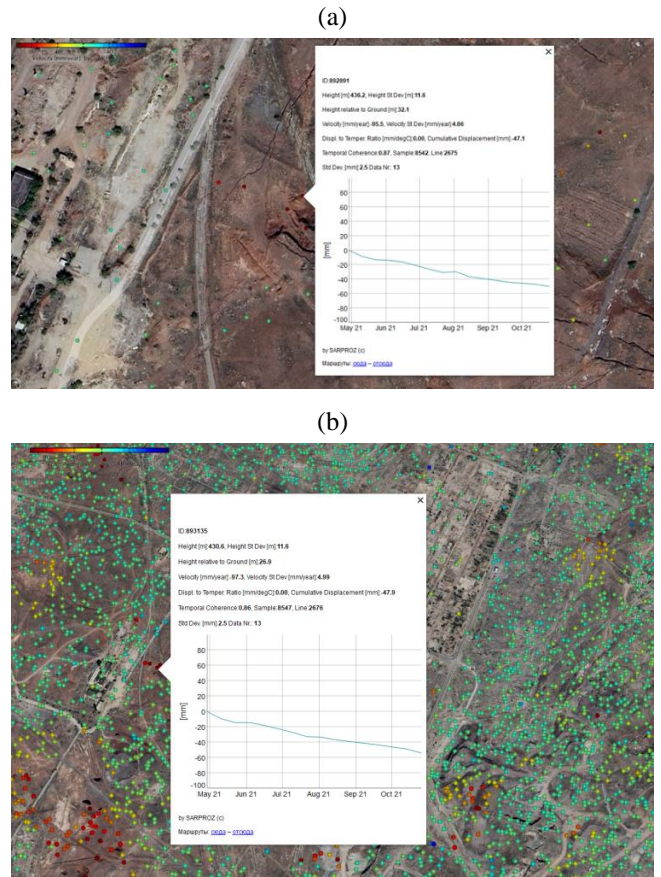
(a)

(b)

Figure 18. Dynamics of displacements of the points of a sinkhole with smooth earth's surface subsidence for the period of April 29 – October 26, 2021: (a) subsidence dynamics of point 892891; (b) subsidence dynamics of point 893135

For this study, the results of each method were determined individually; that has helped provide much better understanding of the field deformations. Different methods to obtain a consistent interpretation of the monitored earth's surface movements were compared.

4.1. Sinkholes with hidden deformations

In case of sinkholes with hidden deformations, none of the monitoring tools could cope fully. Classical geodetic measurements provide discrete information about the observed movements of points. As a result, they typically do not provide spatially and temporally meaningful estimates of the overall range and magnitude of the earth's surface movement over specific periods of interest. Moreover, such measurements are too labour-intensive, and ground points are difficult to maintain for a long period of time.

Seismic events of the "landslide" type were classified as interferences. A typical seismic event was compared visually with a "landslide"-type event; that showed certain differences in the frequency, duration, and nature of the signal. Gradual weakening of rock layers and moisture saturation are the mechanism of rock mass breaking. That explains the smooth subsidence/caving of the overlying strata without obvious seismic signals.

SAR interferometry also failed to detect superintense subsidence. It is possible that the low-resolution Sentiel-1b data are principally unable to detect them [51], [52]. The budget for this research is limited and there is no possibility of purchasing paid images.

Therefore, experiments to determine intense subsidence within the areas of Zhekazgan field are recommended to be carried out using the data from the COSMO-SkyMed and TerraSAR-X spacecraft.

To identify unstable zones with hidden deformations – without previous deformation and seismological signs, it is recommended to develop a three-dimensional geomechanical model of the field. This model allows combining all the parameters in one database that affect the safety of mining operations. It should take into account structural disturbances of the rock mass, which affect negatively the stability [53]-[57]. To build a model of voids, it is necessary to digitize the secondary documents remained in the archive.

4.2. Sinkholes with smooth subsidence

SAR interferometry is an excellent option in case of sinkholes with smooth subsidence and for areal field monitoring in general; moreover, its combination with high-resolution monitoring methods such as GNSS makes it possible to determine the intertwined causes of the earth's surface movement associated with a variety of complex processes.

In general, the satellite interferometry methods are the only currently available technique for areal monitoring of the earth's surface movements. While using information from space data to assess the industrial surface subsidence, it is possible not only to understand better the current geodynamic situation in the area under study but also to monitor the past 30-40 years. Archival satellite images provide the opportunity to analyze the main trends in the earth's surface movement and identify stable deformation characteristics. This, in turn, does not eliminate the need to plan ground-based observations but makes it possible to determine more accurately their location and conduct them less frequently in time and in spatially sparse areas.

5. Conclusions

The paper examines two cases of caving within Zhezkazgan field. The first caving is characterized by a sudden outcropping sinkhole with the emergency damage to the water pipeline, collectors, roads, and power lines. As a result, a whole package of communications (dirt road, water pipeline, power lines) laid as the "green" corridor collapsed. Before the caving, neither satellite interferometry nor seismic monitoring detected any deformation or seismic events. The geomechanical service could neither predict this caving nor warn about the beginning of the dangerous situation development, which was the essence of the incident.

A study of this sinkhole using SAR interferometry data and other observation methods, including high-precision levelling and GNSS observations for different years (2019, 2020, 2021) showed minor subsidence and surface fluctuations of up to 10 mm, which in most cases were within the range of method accuracy. Since the results of SAR interferometry and seismic monitoring did not reveal intensive processes of surface subsidence or previous seismic events associated with the subsequent caving, this sinkhole was classified as the one with hidden deformations.

In the second case, a sinkhole with smooth subsidence is characterized by slow and smooth earth's surface displacements, which makes their long-term monitoring and forecasting possible. These SAR interferometry methods help detect and analyze smooth subsidence of the earth's surface. At the same time, this monitoring method is safe to use and wide-ranging, covering large areas at once. SAR interferometry makes it possible to determine not only the average annual velocity, in contrast to the ground-based discrete methods, but also determines the displacement dynamics, detecting the occurring fluctuations during the entire observation period.

In addition, to verify the SAR interferometry data, GNSS observations were carried out. In general, there is a good convergence of measurement results using the three methods – SAR interferometry, GNSS observations, and high-precision levelling.

Acknowledgements

References

[1] Issatayeva, F.M., Aubakirova, G.M., Maussymbayeva, A.D., Togaibayeva, L.I., Biryukov, V.V., & Vechkinzova, E. (2023). Fuel and energy complex of Kazakhstan: Geological and economic assessment of enterprises in the context of digital transformation. *Energies*, 16(16), 6002. https://doi.org/10.3390/en16166002

[2] Rudko, G.I., Myatchenko, A.V., Isataeva, F.M., & Portnov, V.S. (2018). Geological-economic estimation of Kazakhstan deposits. *Sustainable Development of Mountain Territories*, 10(4), 471-480. https://doi.org/10.21177/1998-4502-2018-10-4-471-480

[3] Akpanbayeva, A., & Issabek, T. (2023). Assessing a natural field of rock mass stress by means of in-situ measurements within Vostochnaya Sary-Oba deposit in Kazakhstan. *Mining of Mineral Deposits*, 17(3), 56-66. https://doi.org/10.33271/mining17.03.056

[4] Aubakirova, G., Rudko, G., & Isataeva, F. (2021). Assessment of metallurgical enterprises' activities in Kazakhstan in the context of international trends. *Economic Annals-XXI*, 187(1-2), 121-130. https://doi.org/10.21003/EA.V187-12

[5] Nurpeisova, M., Bekbassarov, Z., Kenesbayeva, A., Kartbayeva, K., & Gabitova, U. (2020). Complex evaluation of geodynamic safety in the development of hydrocarbon reserves deposits. *News of the National Academy of Sciences of the Republic of Kazakhstan, Series of Geology and Technical Sciences*, (1), 90-98. https://doi.org/10.32014/2020.2518-170X.11

[6] Bozzano, F., Mazzanti, P., Prestininzi, A., & Scarascia Mugnozza, G. (2010). Research and development of advanced technologies for landslide hazard analysis in Italy. *Landslides*, (7), 381-385. https://doi.org/10.1007/s10346-010-0208-x

[7] Minderhoud, P.S., Hlavacova, I., Kolomaznik, J., & Neussner, O. (2020). Towards unraveling total subsidence of a mega-delta–the potential of new PS InSAR data for the Mekong delta. *Proceedings of the International Association of Hydrological Sciences*, (382), 327-332. https://doi.org/10.5194/piahs-382-327-2020

[8] Bischoff, C.A., Ferretti, A., Novali, F., Uttini, A., Giannico, C., & Meloni, F. (2020). Nationwide deformation monitoring with SqueeSAR® using Sentinel-1 data. *Proceedings of the International Association of Hydrological Sciences*, (382), 31-37. https://doi.org/10.5194/piahs-382-31-2020

[9] Rokugawa, S., & Nakamura, T. (2015). Long-range ground deformation monitoring by InSAR analysis. *Proceedings of the International Association of Hydrological Sciences*, (372), 343-346. https://doi.org/10.5194/piahs-372-343-2015

[10] Peter, R., & Jennifer, A. (2005). Technology plan for the terrestrial planet finder interferometer. *JPL Publication 05-5*. Jet Propulsion Laboratory California Institute of Technology Pasadena, California.

[11] Fielding, E.J., Talebian, M., Rosen, P.A., Nazari, H., Jackson, J.A., Ghorashi, M., & Walker, R. (2005). Surface ruptures and building damage of the 2003 Bam, Iran, earthquake mapped by satellite synthetic aperture radar interferometric correlation. *Journal of Geophysical Research: Solid Earth*, *110*(B3). https://doi.org/10.1029/2004JB003299

[12] Tran, D.H., & Wang, S.J. (2020). Land subsidence due to groundwater extraction and tectonic activity in Pingtung Plain, Taiwan. *Proceedings of the International Association of Hydrological Sciences*, (382), 361-365. https://doi.org/10.5194/piahs-382-361-2020

[13] Agudelo, G., Wang, G., Liu, Y., Bao, Y., & Turco, M.J. (2020). GPS geodetic infrastructure for subsidence and fault monitoring in Houston, Texas, USA. *Proceedings of the International Association of Hydrological Sciences*, (382), 11-18. https://doi.org/10.5194/piahs-382-11-2020

[14] Venmans, A.A., Op De Kelder, M., De Jong, J., Korff, M., & Houtepen, M. (2020). Reliability of InSAR satellite monitoring of buildings near inner city quay walls. *Proceedings of the International Association of Hydrological Sciences*, (382), 195-199. https://doi.org/10.5194/piahs-382-195-2020

[15] Gandolfi, S., Macini, P., Poluzzi, L., & Tavasci, L. (2020). GNSS measurements for ground deformations detection around offshore natural gas fields in the Northern Adriatic Region. *Proceedings of the International Association of Hydrological Sciences*, (382), 89-93. https://doi.org/10.5194/piahs-382-89-2020

[16] Abdelsamea, T., Yousef, M.A., Alemam, M.K., & Mostafa, Y.G. (2023). Effect of IGS baseline length on GNSS positioning accuracy. *Rudarsko-Geolosko-Naftni Zbornik*, *38*(3), 81-93. https://doi.org/10.17794/rgn.2023.3.7

[17] Wang, Z., Li, W., Zhao, Y., Jiang, A., Zhao, T., Guo, Q., & Ren, X. (2023). Monitoring ground displacement in mining areas with time-series interferometric synthetic aperture radar by integrating persistent scatterer/slowly decoherent filtering phase/distributed scatterer approaches based on signal-to-noise ratio. *Applied Sciences*, *13*(15), 8695. https://doi.org/10.3390/app13158695

[18] Mendygaliyev, A., Arshamov, Y., Selezneva, V., Yazikov, E., & Bekbotayeva, A. (2021). Prospects for application of multi-spectral earth sensing data in forecasting and searching for reservoir-infiltration uranium deposits. *News of the National Academy of Sciences of the Republic of Kazakhstan, Series of Geology and Technical Sciences*, *2*(446), 90-97. https://doi.org/10.32014/2021.2518-170X.39

[19] Venera, J., Anton, F., Irina, K., & Alena, Y. (2016). SAR interferometry technique for ground deformation assessment on Karazhanbas oilfield. *Procedia Computer Science*, (100), 1163-1167. https://doi.org/10.1016/j.procs.2016.09.271

[20] Kassymkanova, K.K., Istekova, S., Rysbekov, K., Amralinova, B., Kyrgizbayeva, G., Soltabayeva, S., & Dossetova, G. (2023). Improving a geophysical method to determine the boundaries of ore-bearing rocks considering certain tectonic disturbances. *Mining of Mineral Deposits*, *17*(1), 17-27. https://doi.org/10.33271/mining17.01.017

[21] Omirzhanova, Z., Kartbayeva, K.T., Aimenov, A.T., & Jazbayev, A.T. (2017). Geodetic measurements of modern movements of the earth surface on Almaty geodynamic polygon. *International Multidisciplinary Scientific GeoConference*, (17), 337-346.

[22] Sarah, D., Soebowo, E., & Satriyo, N.A. (2021). Review of the land subsidence hazard in Pekalongan Delta, Central Java: insights from the subsurface. *Rudarsko-Geolosko-Naftni Zbornik*, *36*(4), 163-176. https://doi.org/10.17794/rgn.2021.4.13

[23] Hnatushenko, V.V., Mozhovyi, D.K., & Vasyliev, V.V. (2017). Satellite monitoring of deforestation as a result of mining. *Naukovyi Natsionalnoho Hirnychoho Universytetu*, (5), 94-99.

[24] Jakopec, I., Marendić, A., & Grgac, I. (2022). A novel approach to landslide monitoring based on unmanned aerial system photogrammetry. *Rudarsko-Geolosko-Naftni Zbornik*, *37*(5), 83-101. https://doi.org/10.17794/rgn.2022.5.8

[25] Brandt, J.T., Sneed, M., & Danskin, W.R. (2020). Detection and measurement of land subsidence and uplift using interferometric synthetic aperture radar, San Diego, California, USA, 2016-2018. *Proceedings of the International Association of Hydrological Sciences*, (382), 45-49. https://doi.org/10.5194/piahs-382-45-2020

[26] Gee, D., Bateson, L., Sowter, A., Grebby, S., Novellino, A., Cigna, F., & Wyatt, L. (2017). Ground motion in areas of abandoned mining: Application of the intermittent SBAS (ISBAS) to the Northumberland and Durham Coalfield, UK. *Geosciences*, *7*(3), 85. https://doi.org/10.3390/geosciences7030085

[27] Vlasenko, V., Dudlia, K., & Kyrychenko, M. (2019). Mathematical model of the cracking process in the coal-rock massif under hydrodynamic impact. *E3S Web of Conferences*, (109), 00111. https://doi.org/10.1051/e3sconf/201910900111

[28] Seitmuratova, E., Arshamov, Y., Bekbotayeva, A., Baratov, R., & Dautbekov, D. (2016). Priority metallogenic aspects of late Paleozoic volcanic-plutonic belts of Zhongar-Balkhash fold system. *International Multidisciplinary Scientific GeoConference Surveying Geology and Mining Ecology Management*, (1), 511-518. https://doi.org/10.5593/sgem2016/b11/s01.064

[29] Sarybayev, O., Nurpeisova, M., Kyrgizbayeva, G., & Toleyov, B. (2015). Rock mass assessment for man-made disaster risk management. *New Developments in Mining Engineering 2015: Theoretical and Practical Solutions of Mineral Resources Mining*, 403-409. https://doi.org/10.1201/b19901-70

[30] Kyrgizbayeva, G., Nurpeisov, M., & Sarybayev, O. (2015). The monitoring of earth surface displacements during the subsoil development. *New Developments in Mining Engineering 2015: Theoretical and Practical Solutions of Mineral Resources Mining*, 161-167. https://doi.org/10.1201/b19901-30

[31] Utepov, E.B., Omirbai, R.S., Suleev, D.K., Nurgaliev, A.K., & Ibraeva, G.M. (2015). Developing metallic damping materials. *Metallurgist*, *58*(11-12), 1025-1031. https://doi.org/10.1007/s11015-015-0035-3

[32] Liu, J.B., Dai, H.Y., Wang, X., Shynar, A., & Madimarova, G. (2014). Three-dimensional geological modeling of mining subsidence prediction based on the blocks. *Advanced Materials Research*, (905), 697-701. https://doi.org/10.4028/www.scientific.net/AMR.905.697

[33] Nurpeisova, M.B., & Kurmanbaev, O.S. (2016). Laws of development of geomechanical processes in the rock mass Maykain mine. *News of the National Academy of Sciences of the Republic of Kazakhstan, Series of Geology and Technical Sciences*, *6*(420), 109-115.

[34] Aitkazinova, S.K., Derbisov, K.N., Donenbayeva, N.S., Nurpeissova, M., & Levin, E. (2020). Preparing solutions based on industrial waste for fractured surface strengthening. *News of the National Academy of Sciences of the Republic of Kazakhstan, Series of Geology and Technical Sciences*, *5*(443), 13. https://doi.org/10.32014/2020.2518-170X.99

[35] Nurpeisova, M.B., Sarybaiev, O.A., & Kurmanbaiev, O.S. (2016). Study of regularity of geomechanical processes development while developing deposits by the combined way. *Naukovyi Visnyk Natsionalnoho Hirnychoho Universytetu*, (4), 30-36.

[36] Baibatsha, A.B., Bekbotayeva, A.A., & Bekbotayev, A.T. (2015). Ore minerals of Carboniferous copper sediment-hosted Zhezkazgan deposit (Central Kazakhstan). *International Multidisciplinary Scientific GeoConference Surveying Geology and Mining Ecology Management*, (1), 329-335.

[37] Baibatsha, A.B., Bekbotayev, A.T., & Bekbotayeva, A.A. (2013). Ore-bearing strata lithology of the Zhezkazgan copper sandstones deposit. *International Multidisciplinary Scientific GeoConference Surveying Geology and Mining Ecology Management*, (1), 135-140. https://doi.org/10.5593/SGEM2013/BA1.V1/S01.019

[38] Medvedskiy, Yu. (2019). Radiolokatsionnaya interferometriya s sintezirovannoy aperturoy v geodezii. *Inzhenernaya Geodeziya*, (67), 110-122. https://doi.org/10.32347/0130-6014.2019.67.110-122

[39] Wojtecki, Ł., Kurzeja, J., & Knopik, M. (2021). The influence of mining factors on seismic activity during longwall mining of a coal seam. *International Journal of Mining Science and Technology*, *31*(3), 429-437. https://doi.org/10.1016/j.ijmst.2021.01.010

[40] Aitkazinova, S.K., Nurpeisova, M.B., Kirgizbaeva, G.M., & Milev, I. (2014). Geomechanical monitoring of the massif of rocks at the combined way of development of fields. *International Multidisciplinary Scientific GeoConference Surveying Geology and Mining Ecology Management*, *2*(2), 279-292.

[41] Akhmetov, R., Makhmetova, G., Orynbassarova, E., Baltiyeva, A., Togaibekov, A., Roberts, K., & Yerzhankyzy, A. (2022). The study of kinematic GNSS surveying for BIM georeferencing. *The International Archives of the Photogrammetry, Remote Sensing and Spatial Information Sciences*, (46), 7-14. https://doi.org/10.5194/isprs-archives-XLVI-5-W1-2022-7-2022

[42] Herring, T., King, R., Floyd, M., & McClusky, S. (2018). *Introduction to GAMIT/GLOBK*. Manual. Cambridge, United Kingdom: Massachussetts Insitute of Technology.

[43] Zhantayev, Z., Kaldybayev, A., Bibossinov, A., Vilyaev, A., Turgumbayev, A., & Nurakynov, S. (2018). GPS-derived velocity fields of northern Tien Shan from permanent stations in Kazakhstan. *Proceedings of the International Geoscience and Remote Sensing Symposium*, 3189-3191. https://doi.org/10.1109/IGARSS.2018.8518103

[44] Segall, P. (1989). Earthquakes triggered by fluid extraction. *Geology*, *17*(10), 942-946. https://doi.org/10.1130/0091-7613(1989)017<0942:ETBFE>2.3.CO;2

[45] Portnov, V.S., Yurov, V.M., & Maussymbayeva, A.D. (2016). Applied problems of thermodynamic approach to the analysis of geophysical information. *Naukovyi Visnyk Natsionalnoho Hirnychoho Universytetu*, (1), 5-11.

[46] Baltiyeva, A., Shamganova, L., Raskaliyev, A., & Koval, E. (2020). Approval of the domestic development of a software and technical com-

plex for a high-precision satellite positioning system at the Kacharsky open-pit mines. *International Multidisciplinary Scientific GeoConference*, *20*(2.2), 27-34. https://doi.org/10.5593/sgem2020.2.2/s09.004

[47] Lanari, R., Casu, F., Manzo, M., & Lundgren, P. (2007). Application of the SBAS-DInSAR technique to fault creep: A case study of the Hayward fault, California. *Remote Sensing of Environment*, *109*(1), 20-28. https://doi.org/10.1016/j.rse.2006.12.003

[48] Kamza, A.T., Kuznetsova, I.A., & Levin, E.L. (2023). Prediction of the flooding area of the northeastern Caspian Sea from satellite images. *Geodesy and Geodynamics*, *14*(2), 191-200. https://doi.org/10.1016/j.geog.2022.08.003

[49] Han, Y., Liu, G., Liu, J., Yang, J., Xie, X., Yan, W., & Zhang, W. (2023). Monitoring and analysis of land subsidence in Jiaozuo City (China) based on SBAS-InSAR technology. *Sustainability*, *15*(15), 11737. https://doi.org/10.3390/su151511737

[50] Yun, A., Terentyeva, I., & Bochkareva, T. (2015). The choice of the concept of stabilization of the geomechanical situation at the Zhezkazgan field. *Surveying Bulletin*, (2), 47-52.

[51] Simmons, B.S., & Wempen, J.M. (2021). Quantifying relationships between subsidence and longwall face advance using DInSAR. *International Journal of Mining Science and Technology*, *31*(1), 91-94. https://doi.org/10.1016/j.ijmst.2020.12.021

[52] Smigaj, M., Hackney, C.R., Diem, P.K., Ngoc, N.T., Du Bui, D., Darby, S.E., & Leyland, J. (2023). Monitoring riverine traffic from space: The untapped potential of remote sensing for measuring human footprint on inland waterways. *Science of the Total Environment*, (860), 160363. https://doi.org/10.1016/j.scitotenv.2022.160363

[53] Yan, W., Guo, J., & Yan, S. (2023). Difference in surface damage between deep and shallow mining of underground coal resources in China. *Sustainability*, *15*(9), 7296. https://doi.org/10.3390/su15097296

[54] Sedina, S., Berdinova, N., Abdikarimova, G., Altayeva, A., & Toksarov, V. (2021). Numerical modeling of the stress-strain state of the kurzhunkul open-pit mine. *News of the National Academy of Sciences of the Republic of Kazakhstan, Series of Geology and Technical Sciences*, *6*(450), 110-117. https://doi.org/10.32014/2021.2518-170X.126

[55] Khanal, M., Adhikary, D., & Balusu, R. (2012). Numerical analysis and geotechnical assessment of mine scale model. *International Journal of Mining Science and Technology*, *22*(5), 693-698. https://doi.org/10.1016/j.ijmst.2012.08.017

[56] Ivadilinova, D.T., Issabek, T.K., Takhanov D.K., & Yeskenova G.B. (2023). Predicting underground mining impact on the earth's surface. *Naukovyi Visnyk Natsionalnoho Hirnychoho Universytetu*, (1), 32-37. https://doi.org/10.33271/nvngu/2023-1/032

[57] Kozhogulov, K.C., Takhanov, D.K., Kozhas, A.K., Imashev, A.Z., & Balpanova, M.Z. (2020). Methods of forward calculation of ground subsidence above mines. *Journal of Mining Science*, *56*(2), 184-195. https://doi.org/10.1134/S1062739120026637

Дослідження провалів земної поверхні з використанням радарної супутникової інтерферометрії на прикладі Жезказганського родовища, Казахстан

А. Балтієва, Е. Оринбасарова, М. Жараспаєв, Р. Ахметов

Мета. Дослідження спрямоване на оцінку потенціалу радарної супутникової інтерферометрії (РСА-інтерферометрії) в аналізі та прогнозі зсувів земної поверхні.

Методика. В рамках цього дослідження виконано аналіз попередніх інструментальних спостережень, таких як високоточне нівелювання та сейсмомоніторинг. Проведено спостереження із застосуванням глобальних навігаційних супутникових систем (ГНСС), а також опрацьовано супутникові знімки за допомогою методу послідовної інтерферометрії постійних розсіювачів радарного сигналу (РС).

Результати. Результати дослідження підтвердили схожість між даними, отриманими за допомогою наземних інструментальних методів та даними, отриманими із використанням супутникової інтерферометрії. Було виділено два типи провалів земної поверхні, а саме: провали з плавним осіданням і приховані деформації, які не супроводжуються попередніми деформаційними чи сейсмологічними ознаками. Осідання з плавним характером успішно контролюються та прогнозуються за допомогою методів РСА-інтерферометрії. Також було представлено алгоритм прогнозування лінійних трендів зміщень різних часових інтервалах за допомогою методу скінченних елементів.

Наукова новизна полягає у комплексному характері проведення дослідження, що охоплює порівняльний аналіз різних методів моніторингу, вивчення різних типів провалів, виявлення обмежень існуючих методів, а також у пропозиції нових підходів для більш точного та об'єктивного аналізу деформацій земної поверхні на родовищі.

Практична значимість. Результати цього дослідження мають практичну значущість для геомеханіків та операторів гірничих робіт. Вони можуть використовувати ці дані для моніторингу й управління обвалами земної поверхні, забезпечуючи безпеку персоналу та зберігаючи наземну інфраструктуру, де це можливо.

Ключові слова: провали, земна поверхня, підземні порожнечі, РСА-інтерферометрія, прогноз